Society for Science and Education
United Kingdom

ISSN: 2055 - 1266
Volume 5 No 3
June 2018

Journal of Biomedical Engineering and Medical Imaging

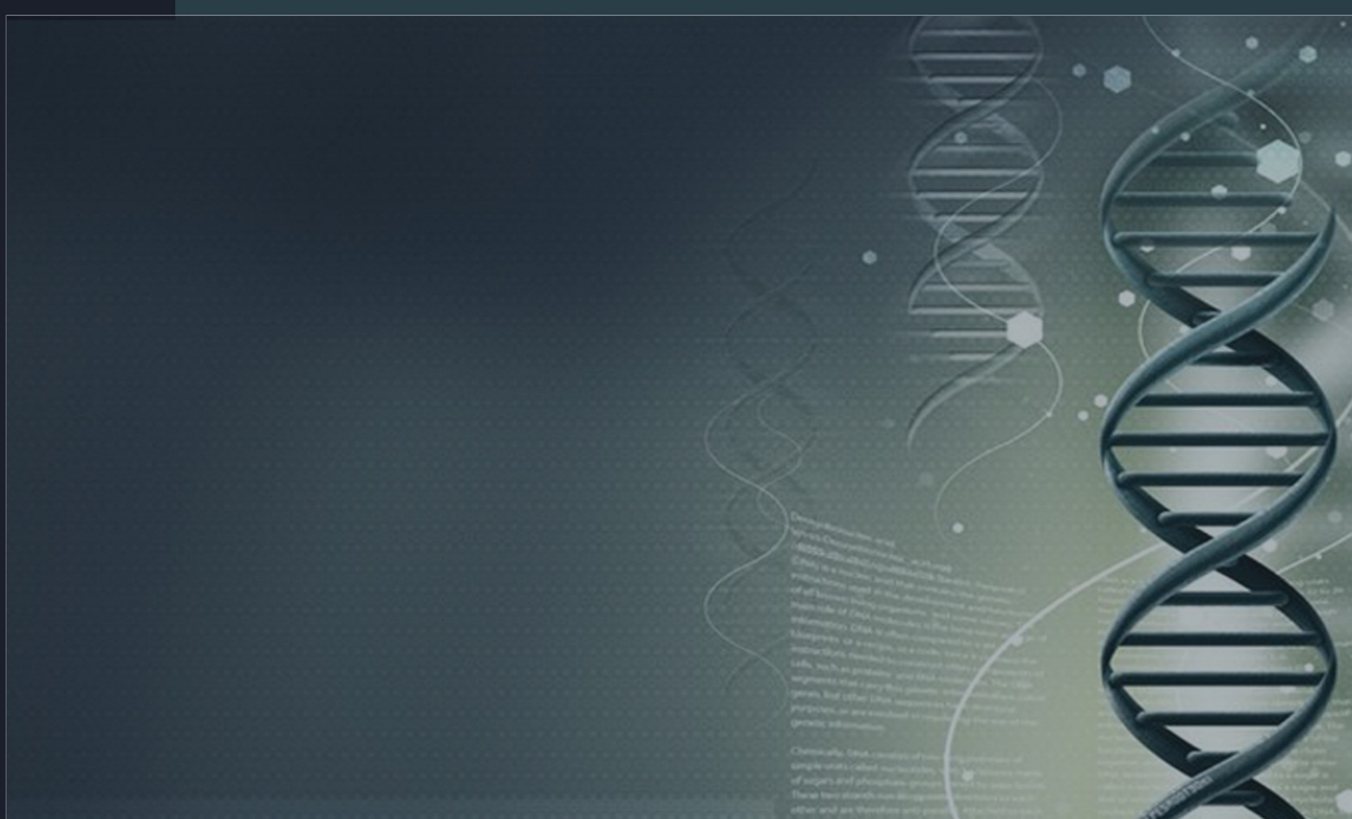

TABLE OF CONTENTS

EDITORIAL ADVISORY BOARD

DISCLAIMER

SOCIETY FOR SCIENCE AND EDUCATION UNITED KINGDOM

JBEMi JOURNAL OF BIOMEDICAL ENGINEERING AND MEDICAL IMAGING

ISSN: 2055-1266
VOLUME 5 ISSUE 3

Implementing Archimedean Spiral Approach to Evaluate Left Ventricular Myocardial Functions

Yashbir Singh[1], Deepa[1], Shi Yi Wu[1], Michael Friebe[2], Joao Manuel R. S. Tavares[3], Hu Wei-Chih[1]

[1]*Department of Biomedical Engineering, Chung Yuan Christian University, Zhongli, Taiwan*

[2]*Electrical Engineering and Information Technologies, Otto-von-Guericke-University, Magdeburg, Germany*

[3]*Instituto de Ciência e Inovação em Engenharia Mecânicae Engenharia Industrial, Departamento de Engenharia Mecânica, Faculdade de Engenharia, Universidade do Porto, Porto, PORTUGAL*

yashbir143@gmail.com; weichihhu@gmail.com; weichihhu@cycu.edu.tw

ABSTRACT

Heart disease can be determined by the calculating regional and global wall motion of the left ventricular (LV). In this research, we designed a dynamic simulation tool using Computed Tomography (CT) images that helps to find the difference between actual and simulated left ventricular functions. In this study, thirteen healthy subjects were involved with actual and simulated left ventricular functions. We obtained the high correlation between actual left ventricular wall motion (ALVWM) and simulated left ventricular wall motion (SLVWM) which is (r = 0.99). Our results validate that our simulation tool is feasible for simulating left ventricular motion.

Keywords: Left-Ventricular remodeling, left ventricular wall motion, Archimedean spiral, Myocardial functions, Computer Tomography.

1 Introduction

Cardiovascular disease has recognized as the leading causes of death in the entire world. WHO report suggest that 17.7 million people died from CVDs in 2015, representing 31% of all global deaths. Approx 7.4 million were died due to coronary heart disease and 6.7 million were due to stroke. In 2013 there were >54 million deaths globally because of CVDs. The majority of CVD deaths were attributable to either ischemic heart disease (IHD). Over the last few decades, chronic diseases such as cardiovascular disease (CVD), have accounted for a significant fraction of death tolls worldwide. It is well known that smoking, obesity, blood pressure and diabetes mellitus are major risk factors for CVD [1]. In addition, it has also been recognized that many CVD risk factors are associated with each other. It is also seen that heart wall motion can be an indicator for predicting cardiovascular disease in groups of patients with myocardial infarction (MI), unstable angina, typical chest pain, and congestive heart failure (CHF) [2]. left ventricular contractile abnormalities can be an important manifestation of coronary artery disease. These wall motion changes may represent ischemia or infarction of myocardium [3]. This study has been performed to calculate wall motion between actual and simulated LV wall motion and to show correlation study between endocardial displacements to the central axis.

DOI: 10.14738/jbemi.53.4497
Publication Date: 10th May 2018
URL: http://dx.doi.org/10.14738/jbemi. 53.4497

2 Methods

The objective of this research was to simulate LV functions and to access local left ventricular myocardial function.

In house developed program was integrated with OpenGL library as a tool for analyzing 4D cardio CT image data set. Images were obtained from the computerized tomography (CT) SIEMENS_LEOVB30B instrument provided by Taipei Veterans General Hospital. This study and the informed consent procedure were approved by the Institutional Review Board of Taipei Veterans General Hospital. In this research, thirteen subjects were involved with atrial fibrillation and left ventricular motion abnormalities. Each subject has 10 sets of timing frames, including a complete heartbeat cycle. The scanned image size was 512 × 512 (pixels). The images were read by the program and confirmed the format for the DICOM (Digital Imaging and Communications in Medicine) and stored in 512x512 gray formats. 3D reorganization and image information was obtained to construct the stereoscopic model of the thoracic area. We set the left ventricular central axis and image was resampled. The left ventricle region was segmentated to enhance the Eigen value of the left ventricular edge. After that, each layer of the image was multiplied by the resample length, breadth resolution and actual layer of thickness. Endometrium was divided into 31 layers and each layer again divided into 930 points in which 30 points have been taken for our study considering 31st layer as the reference layer. After setting the angle and height, we obtained actual left ventricular information at time 0 and calculated the rate of radius change to simulate left ventricular motion. We performed the analysis of the total volume and RVC (rate of volume change)[4,5].

i) We used manually cutting of LV images from base to apical from the entire data set. One image was selected from the dataset and one seeded point was set to start this process. We obtained the geometrical center that connects each slice on long axis, applied regression calculation to find the line as a reference axis for LV (Fig.1) [6] .

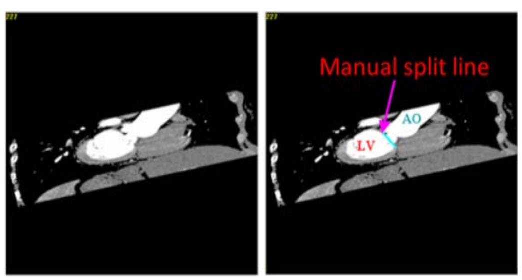

Figure 1. Manually separated line between left ventricle and the aorta

ii) The left ventricular endocardial circle was used for the regional growth of the image which located near to the edge of the image. The regional growth was required to set up the initial seed point. The initial point of the first slice was considered as the reference point of the second slice, the second reference point was set as the seeded region for other layers simultaneously (Fig 2). It was necessary to confirm that the seeded spots of each layer are in the endometrial region and if not, we need to manually correct the seed points [7,8].

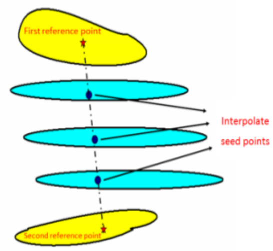

Figure 2. Seeded point star from the first layer and the last layer

iii) In the simulation of left ventricular motion, we got ten sequence of the LV segment from mitral valve to the apical part which represent the distance of the long axis of the left ventricle. Left ventricle contracts with the long axis shorten and the myocardium twist towards the leftward direction then LV wall exhibit thick. The left ventricular end diastolic radius rates of change were calculated. The rate of change in radius and torsion angle were linearly divided into each degree of torsion then the LV contraction model developed shorten axis LV model and radius change torsion model.

iv) Left ventricular systolic contraction describes a uniform movement and relates to the Archimedean spiral equation. Archimedes spiral equation is mentioned below, each θ value has a corresponding r, and the different values of θ correspond to different r values (cot α ≠ 0). If cot α> 0, the curve converges would near the pole when θ approaches to ∞, if cot α <0, θ approaches -∞, when applying the left ventricular simulated motion, the larger the angle of contraction changes in the larger amount. However, considering the ratio of the change of the inner r value of the Archimedes spiral at 180 degrees is too small then turn the angle of twist by 180 degrees (Fig.3) [9].

$$\gamma = ae^{\theta cot\alpha} \tag{1}$$

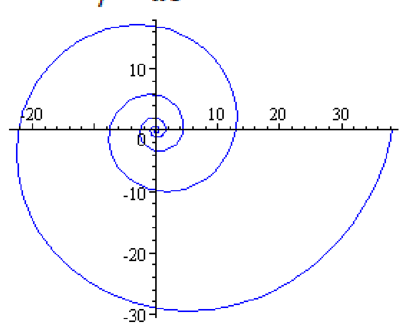

Figure 3. Archimedean Helix

v) The radius rate change was calculated by taking average of the 30 sampling points to the center of each layer and also calculated the actual average final radius of contraction. Whenever a twist occurs, the mean radius of end-diastole and R rate = (RED radius of end-diastole -RES) / RED because we set the maximum twist angle to 20 degrees as shown in equation (ii). The red is the spiral created by the original Archimedes and the blue is by adding a spiral of rate of change in radius. It shows that the radius of the blue line will vary more widely with the angle (Fig.4) [10] .

$$R = \gamma \times (1 + (\frac{R_{rate}}{20} \times angle)) \tag{2}$$

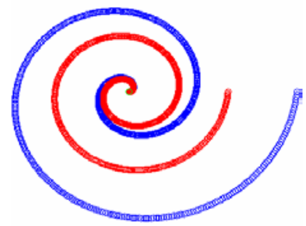

Figure 4. Archimedean spirals plus situational change rates.

Left ventricle before and after the simulation is shown in the figure. A1 represents the right half of the point and A2 represents the left half of the point. The left and right sides of A2 and the left hemisphere makes a distance contraction change in the way to the left, the left ventricle after simulation (A1) and A2 Points change to B1 and B2 respectively (Fig.5).

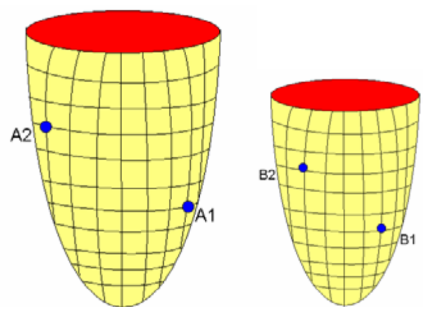

Figure 5. Left ventricle simulation (A1 and A2 before the displacement, Angle and height changes to B1 and B2

3 Results

We proposed a novel approach to evaluate the left ventricular myocardial functions and the normalized wall thickness, which can be used to detect wall motion abnormality. This feature considers the variations between normal and abnormal contraction by tracking the normalized thickness of all segments between the endo and epicardium during the whole cardiac cycle. In this work, the simulated data was validated against real data. The volume difference in each time frame and data set was evaluated. Here we have discussed the result in different steps.

Simulation Interface:

The input parameters shown in the red box. The simulation was performed on 1 degree interval and one-time left-heart grid modeled with 0 to 20 degrees of variation. Each simulated angle is shown in green box (Fig 6) (Fig 7).

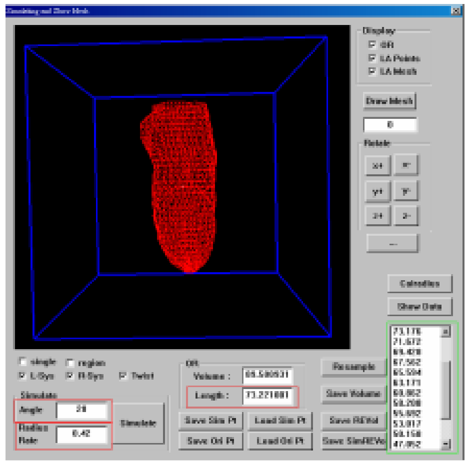

Figure 6. Red box is shown angle and radius rate, Green box is shown long axis parameter. Simulated volume is shown on 0 to 20 degrees

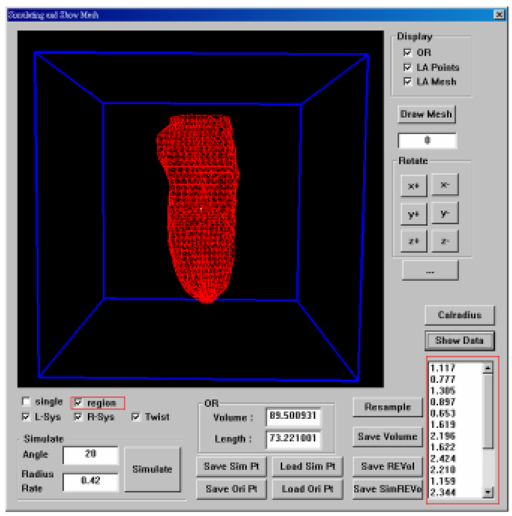

Figure 7. Red box is shown the volume of the local 18 regions.

Parameter Analysis Display Interface

Comparison of the left ventricular function is shown. The red line represents actual VTC and RVC while the green line represents the simulated value. This observation window clearly shows that similarity between the constructed simulation system and the real left ventricle. This confirms the relevance of our system for global left ventricular function between simulated and real left ventricular changes in motion (Fig.8) .

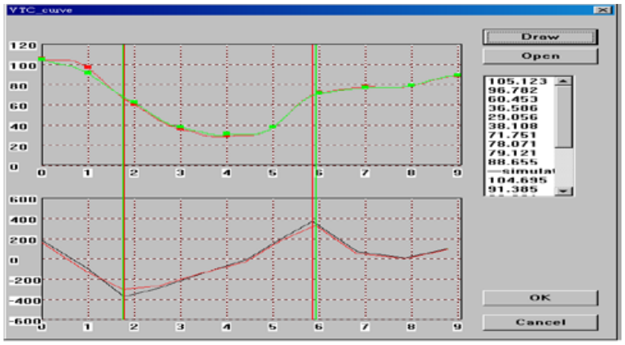

Figure 8. RVC and VTC display interface (red line) as real data (green line) as analog data

Dynamic and Analysis Display Interface

The dynamic interface allows observing more clearly actual and simulated left ventricular motion.

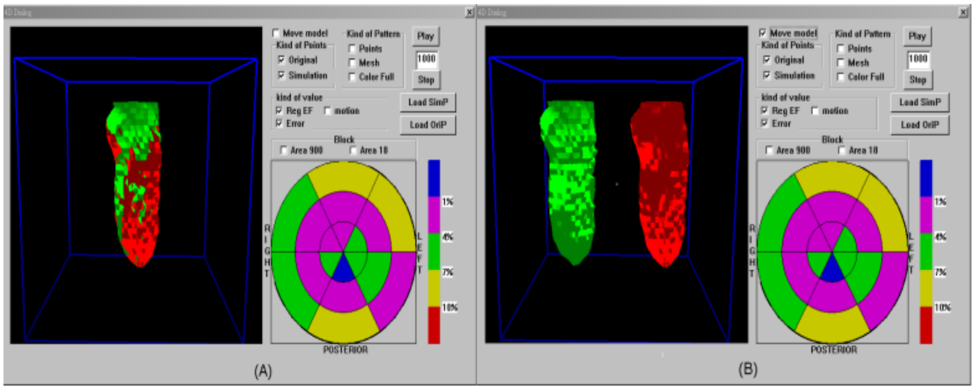

Figure 9 Dynamic Interface (A) Actual vs. Simulated Left Ventricle (B) Separated Actual vs Simulated Left Ventricle

In the comparative study of actual and simulated heart, we got the variation on longitudinal axis which is 1% (purple), 4% (green),7% (green) and 10% (red) on various points of heart wall (Fig.9).

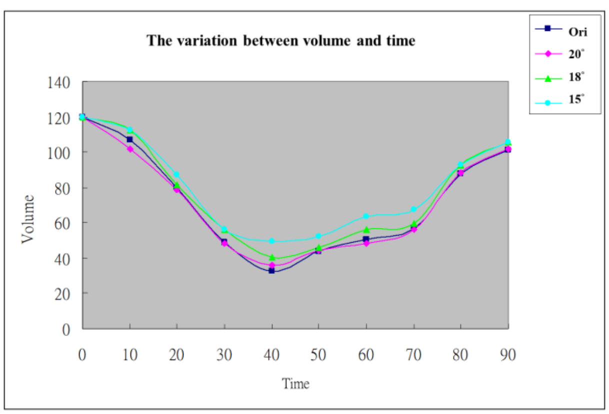

Figure 10. Angle and volume changes in the relationship diagram

This is an initial step to recognize local and global dysfunction in the heart. This study tested the effect of torsion angles which were set at 15^0 (cyan), 18^0 (green), and 20^0 (purple) (Fig.10). The magnitude of left ventricular volume change is relatively smaller when the angle of the input is smaller as well. The calculation of left ventricular function may cause misjudgment. Therefore, we set the torsion angle to 20^0 in order to meet the change of real left ventricular volume (Table1,Table 2).

Table 1 The radius change of 13 subjects

Subject	Radius rate of change	Subject	Radius rate of change
Subject1	0.48	Subject8	0.41
Subject2	0.46	Subject9	0.33
Subject3	0.30	Subject10	0.44
Subject4	0.42	Subject11	0.43
Subject5	0.32	Subject12	0.39
Subject6	0.45	Subject13	0.37
Subject7	0.47		

Table 2. left ventricular volume differences

Time	Original (ml)	Resample (ml)	Difference (ml)
00	134.5	132.4	2.1
10	114.1	112.3	1.8
20	77.3	76.1	1.2
30	46.7	45.9	1.2
40	40.7	40.1	0.6
50	56	55.1	0.9
60	84.1	82.8	1.3
70	96.1	94.6	1.5
80	104.1	102.5	1.6
90	116.8	114.9	1.9

4 Conclusion

In this research, we developed simulation tool using 3D images of actual left ventricular on long-axis changes that tool helps in the accurate assessment of cardiac regional function. We evaluated the difference between the actual and simulated left ventricular function. The difference with the simulated model shows to assess the myocardial position of LV and shown using the myocardial twisting function and shortening of long axis can accurately simulate the LV function. Further research will involve the integration of the heart motion, validating geometrical landmarks and integration of the motion matching.

REFERENCES

[1] Kones, R. Primary prevention of coronary heart disease: integration of new data, evolving views, revised goals, and role of rosuvastatin in management. A comprehensive survey. Drug design, development and therapy, 2011.

[2] Cicala, Silvana, et al. "Prevalence and prognostic significance of wall-motion abnormalities in adults without clinically recognized cardiovascular disease: the Strong Heart Study." Circulation, 2007.

[3] Park, J., Metaxas, D., Young, A., & Axel, L. Model-based analysis of cardiac motion from tagged MRI data. In Computer-Based Medical Systems, 1994., Proceedings 1994 IEEE Seventh Symposium on (pp. 40-45). IEEE. 1994.

[4] Monga and N. Ayache. From voxel to curvature. IEEE Computer Vision and Pattern Recognition, 1991, 644-649.

[5] P. T. Sander and S. W. Zucker. Inferring surface trace and differential structure from 3D images. IEEE Transactions on Pattern Analysis and Machine Intelligence, 1990, 12(9):833-854.

[6] J. Park, D. Metaxas, A. A. Young, and L. Axel, "Deformable models with parameter functions for cardiac motion analysis from tagged MRI data, "IEEE Transactions on Medical Imaging, 1996.

[7] J. Huang, D. Abendschein, V. G. Davila-Roman, and A. A. Amini, "Spatio-temporal tracking of myocardial deformations with a 4-D B-spline model from tagged MRI," IEEE Transactions on Medical Imaging, 1999.

[8] Adams R, Bischof L. Seeded Region Growing. IEEE Transactions on pattern analysis and machine intelligence 1994: 16:641-647.

[9] Walser, H.; Hilton, P.; Pedersen, J.; Mathematical Association of America. Symmetry. Mathematical Association of America. p. 27. ISBN 9780883855324. Retrieved 2014-10-06.

[10] Kass, M., Witkin, A., & Terzopoulos, D. Snakes: Active contour models. International journal of computer vision, 1(4), 1998.

SOCIETY FOR SCIENCE AND EDUCATION UNITED KINGDOM

JBEMi JOURNAL OF BIOMEDICAL ENGINEERING AND MEDICAL IMAGING

ISSN: 2055-1266
VOLUME 5 ISSUE 3

NodeMCU in Patient's Data Transfer to IoT Platform

[1]Tchapga Tchito Christian, [2]Tchiotsop Daniel, [3]Fomethe Anaclet

[1]*College of Technology, University of Buea, Buea, Cameroon;*

[2]*College of Technology Fotso-Victor, University of Dschang, Bandjoun, Cameroon;*

[3]*Faculty of Science, University of Dschang, Dschang, Cameroon;*

tchapga.christian@ubuea.cm; daniel.tchiotsop@gmail.com; safomethe@yahoo.fr

ABSTRACT

Telemedicine is the use of advanced telecommunication tools, within the framework of clinical health, to diagnose diseases or deliver care remotely. In the field of telecommunication, many progress have been made specially with the expanding paradigm of Internet of Things. Our goal in this paper is make use of those low cost and open source tools to accurately transmit patient's parameter to IoT platforms in order to apply a further processing techniques for remote disease diagnostic. To tackle this issue, we made use of ECG samples, sensor for temperature and humidity, connected to the NodeMCU which is one of the fast expanding and effective tools to easily establish communication with large scale data storage servers. The NodeMCU is used to push medical parameters to the ThingSpeak which is one of the most advanced IoT platform embedding MatLab. We made use of two main Application Program Interface (API): Message Queuing Telemetry Transport (MQTT) to push data to server, and the REpresentational State Transfer (REST), web services provide interoperability between computer systems on the Internet. As result of that experimentation we succefully transmited the three parameters, necessary on heart disease diagnosis. This tiny setup could be of a great help for remote medical data processing, also the IoT platform selected gives room to MatLab thereby could allow any type of further and powerful processing.

Keywords: Internet of Things (IoT); NodeMCU; API; REST; MQTT; ECG.

1 Introduction

Telemedicine is the use of telecommunication and information technology to provide clinical health care from a distance. It has been used to overcome distance barriers and to improve access to medical services that would often not be consistently available in distant rural communities. Telemedicine can be beneficial to patients in isolated communities and remote regions, who can receive care from doctors or specialists far away without the patient having to move to visit them [1]. Recent developments in Information Communication Technology can allow healthcare professionals in multiple locations to share information and discuss patient's issues as if they were in the same place. These technologies permit communications between patient and medical staff with both convenience and fidelity, as well as the transmission of medical, imaging and health informatics data from one site to another. Various specialties are contributing to telemedicine, in varying degrees. Just to name some few, in

DOI: 10.14738/jbemi.53.4358
Publication Date: 18th May 2018
URL: http://dx.doi.org/10.14738/jbemi. 53.4358

Telecardiology electrocardiographs, can be transmitted using telephone, mail and wireless Specialist care delivery. Telepsychiatry, Teleradiology, Telepathology, Teledermatology, Teledentistry, Teleaudiology, Teleophthalmology [2]. According to Grigsby [1], there are four suggested types of telemedicine applications: (a) management of specific diseases, (b) use within specific, specialties, (c) classification according to technology, and (d) types of clinical problems. Whitten et al [3] provides a literature review and overviews three proposed evolutionary stages for telemedicine to date, namely synchronous versus asynchronous modalities, data transfer and storage, and automating decision making and robotics.

As More than three-quarters of cardiovascular diseases deaths occur in low- and middle-income countries, the main causes being the lack of cardiologists and equipment in medical centres. A Holter monitor is a battery-operated portable device that measures and records the heart's activity (ECG) continuously for 24 or longer depending on the type of monitoring required. Some devices to acquire ECG signal and enables monitoring patient remotely rather than keeping them in emergency care due to the lacking of expensive ECG devices for developing countries have been developed but using e-mail as transmission mean [4]. Many existing systems have attempted to simplify ECG data acquisition and analysis. These systems utilize other wireless standards such as Wi-Fi [5], Ethernet [6], [7], Bluetooth [7], ZigBee [8], parallel port [9], USB [10] and even GSM [11], [12], [13]. Mbiadoun et al [14] developed a Universal Module of Acquisition and Transmission of Electrophysiological Signal, he focused on phonocardiogram data acquisition and noise cancellation. Although many wireless standards can be used, there are important considerations such as range, throughput, security, ease of implementation and cost. From his research, Hangsik Shin [15] found that the ambient temperature could induce a difference between HRV(heart rate variability) and PRV (Pulse rate variability). The differences were found in the short-term variables that reflect the parasympathetic activity, for this experiment he has to monitor the ECG and photoplethysmography (PPG) under temperature-controlled, constant humidity conditions.

The Internet of Things (IoT) is an abstraction where by each identifiable object can exchange data among each another, with the traditional wired and wireless technologies, and evolving interoperable information and communication technologies, Machine-to-Machine communications (M2M), right up to IoE (Internet of Everything) [16] [17]. Moreover, IoT is a promising paradigm to integrate several technologies and communication solutions. As defined by European Commission Information Society, the Internet of Things is a manageable set of convergent developments in sensing, identification, communication, networking, and informatics devices and systems [18], [19]. Applications of IoT is now extended to several domains like lightning systems [20], Home automation [21], robotics [22] , health domain [23], environmental science [24] and so on… Some authors have successfully coupled IoT with PWM especially in telecoms [17] and also applied in IOC (Internet on a chip) in robots [22]. Tchamda et al [25] developed a Medical systems for telemonitoring of Heart's mechanical activity and Goelocalization of the Patient Based on the MQTT API. A website uses a URL address to make a call to a server and pull up a webpage in a browser. APIs also facilitate calls to a server, but they execute it more simply. They connect the web, allowing developers, applications, and sites to tap into databases and services much like open-source software. APIs do this by acting like a universal converter plug offering a standard set of instructions

There are many types of APIs. One of the most common types of APIs are Web APIs; these APIs, otherwise known as Web Services, provide an interface for web applications, or applications that need to connect to each other via the Internet to communicate. There are tens of thousands of public APIs that can be used to do everything from checking traffic and weather, to updating your social media status, or even to make payments. There are hundreds of thousands more private Web APIs. These APIs are not available to be consumed by the general public; rather, they are used by companies to extend their services and capabilities across a broad range of use cases.

This work is divided in two main parts. The first one is all about Material and method employed, where we invocated two subparts of our embedded system, namely the hardware section and the software section. The second section is dedicated the implementation of the first part. Thereafter, we will conclude and announce perspectives.

2 Material and Methods

Under the paradigm of IoT and eHealth (eHealth is the use of information and communication technologies (ICT) for health), we will develop in this section a solution to ease ECG data transfer for further processing, by allowing a more powerfull processing tool like matLab to display some ECG data sampled real time. To do so we take advantage of ThingSpeak which is an open IoT platform with MATLAB analytics. Moreover, IoT is a promising paradigm to integrate several technologies and communication solutions. The Internet of Things is a manageable set of convergent developments in sensing, identification, communication [16] [17], networking, and informatics devices and systems [18], [19]. The brain behind the set is the NodeMCU ESP8266. This device will take advantage of a Wi-Fi network. We are going to display via a given network, some ECG strips, through an embedded server, inward a single tiny device. This approach free us from the use of urge systems like dedicated server, router, wires, connectors etc…

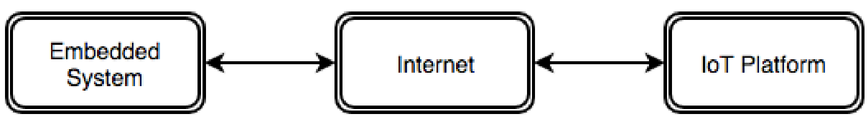

Figure 1 Main Modules for IoT Biomedical system

MQTT is a publish/subscribe architecture that is developed primarily to connect bandwidth and power-constrained devices over wireless networks. It is a simple and lightweight protocol that runs over TCP/IP sockets or WebSockets. MQTT over WebSockets can be secured with SSL. The publish/subscribe architecture enables messages to be pushed to the client devices without the device needing to continuously poll the server.

REST is the short form of Representational State Transfer. As shown it is built on HTTP/TCP layers. The REST protocol uses bus based architecture, where in no broker component is needed and end devices can communicate directly. In this request and response messages are used between end devices to exchange the information

ThingSpeak is an IoT platform that uses channels to store data sent from apps (Android, IOs…) or devices. With the settings described in Channel Configurations, we can create a channel, then send data to a channel, and retrieve data from a given channel. For this paper, we made our channels public to be able to share data, with some other medical doctors or hospital around the world. Using the REST API calls such as GET, POST, PUT, and DELETE, helped us create a channel and update its feed, update an existing channel, clear a channel feed, and delete a channel. we made use of the MQTT Publish method to update a channel feed.

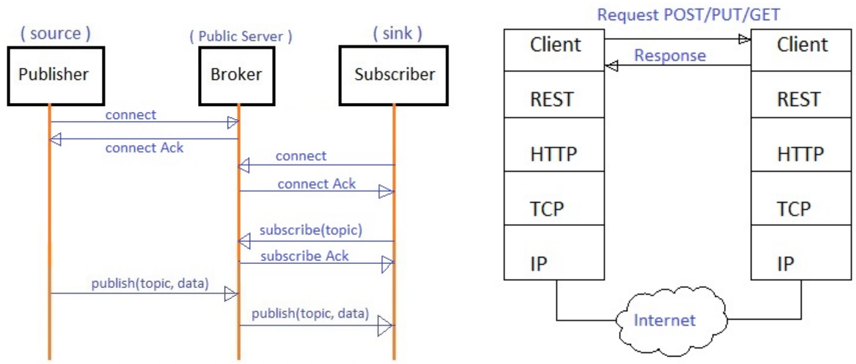

(a) (b)

Figure 2: a) Broker based MQTT Protocol, b) REST Protocol

MATLAB® analysis and visualization apps enabled us to explore and view our channel data. ThingSpeak enables is able to interact with social media, web services, and devices through APIs: REST and MQTT. REST API uses calls to create and update ThingSpeak channels and charts. MQTT API is used to update ThingSpeak channels

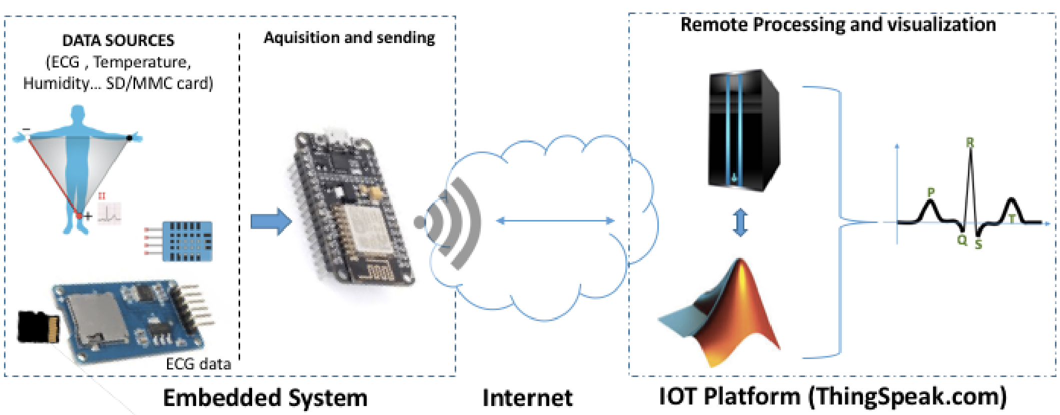

Figure 3: Main Elements for the IoT Biomedical system's architecture

The architecture proposed in **Error! Reference source not found.**, is a benchmark to illustrate our methodology. ECG data collected initially and stored in flash memory, could be inserted into a MMC shield, connected to NodeMCU. This small embedded system converted to Client for Internet can therefore be connected to the thingspeak platform via the wifi layer and transfer those records to the platform. The MatLab machine embedded into thingSpeaktm is then used to carry out further processing

This section is actually divided in two mains sub-sections the first part is all about putting all the hardware together with few adjustments, the second part is all about programming the ESP8622 in Lua language, and Android programing.

2.1 Hardware Design

The new ESP8266 has captured the attention of professional designers, and it has the potential to be an asset in the internet of things. It is highly integrated circuit consists of a 32-bit RISC processor. The ESP8266 also includes a built-in 802.11 b/g/n Wi-Fi circuit that is ready to be directly connected to an antenna engraved on its board. Engineered for mobile devices, wearable electronics and IoT applications, ESP8266EX achieves low power consumption with a combination of several proprietary technologies .

We have two versions of the DHT sensor, they look a bit similar and have the same pinout, but have different characteristics. Here are the specifications of the DHT: Ultra low cost, 3 to 5V power and I/O, 2.5mA max current use during conversion (while requesting data), Good for 20-80% humidity readings with 5% accuracy Good for 0-50°C temperature readings ±2°C accuracy, No more than 1 Hz sampling rate (once every second). Especially DHT22 is Good for 0-100% humidity readings with 2-5% accuracy, Good for -40 to 80°C temperature readings ±0.5°C accuracy, No more than 0.5 Hz sampling rate (once every 2 seconds). The DHT sensor includes a resistive-type humidity measurement component and a NTC temperature measurement component, and connects to a high performance 8-bit microcontroller, Measurement Range for humidity [20%;90%] RH, Humidity Accuracy ± 5% RH, Temperature Accuracy ± 2°C.

The DS18S20 digital thermometer provides 9-bit Celsius temperature measurements. It communicates over a 1-Wire bus that by definition requires only one data line (and ground) for communication with a central microprocessor. Each DS18S20 has a unique 64-bit serial code, which allows multiple DS18S20s to function on the same 1-Wire bus. Thus, it is simple to use one microprocessor to control many DS18S20s distributed over a large area. Measures Temperatures from -55°C to +125°C, ±0.5°C Accuracy from -10°C to +85°C.

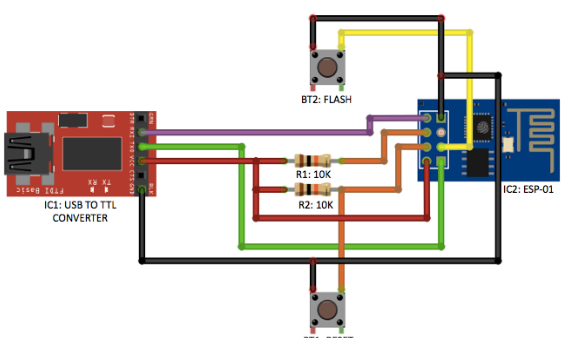

Figure 4:Programming environment

2.2 Software Design

REST is a representational state transfer architectural style designed as a request/response model that communicates over HTTP. MQTT is a publish/subscribe model that runs over TCP/IP sockets or WebSockets. MQTT over WebSockets can be secured with SSL. It is possible to update data to a ThingSpeak™ channel either using a REST GET or POST request or using MQTT PUBLISH method. You retrieve channel data using a REST GET request or MQTT SUBSCRIBE [26]. It is useful to use REST calls to update or retrieve data from a ThingSpeak channel. It is useful to use MQTT to update data to a

ThingSpeak channel, when the device is power-constrained, and requires lower battery consumption to send data to ThingSpeak. Also, an MQTT PUBLISH operation is typically faster in this scenario, when the device connectivity is intermittent, and has limited bandwidth usage, when the immediate updates of data posted to a channel.

The flow chart in **Error! Reference source not found.** summarizes the global functioning, of the system. As the embedded system connects to IoT platform's server, it gets identified, then upload data to the correct channel, then disconnect later after a while, then restarts the cycle.

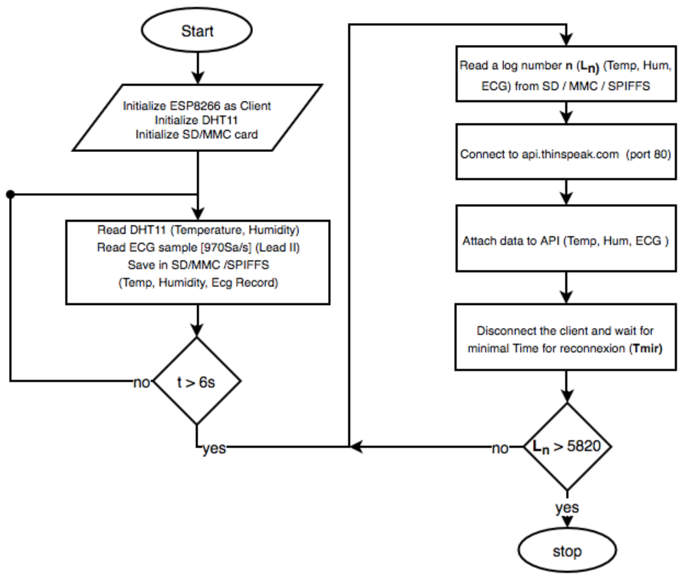

Figure 5: Flow chart illustrating software implementation

The flow chart developed in **Error! Reference source not found.** shows that when the system is started, the NodeMCU is initialised and set as client, as well as the DHT11, for temperature and humidity, the storage device considered for this architecture is an external Multimedia Card, in case that large data initially kept in such a device is to be transferred. Thereafter, in case of direct acquisition, for a device able to acquire at 970 Samples per second, we can keep those record, either in the MMC card previously initialised or in the internal memory of the NodeMCU. A common length of an ECG printout is 6 seconds, known as a "six second strip". Later the system loops through the data acquired to push them to the IoT platform. Read the next sample, connect to the API via port 80, gather temperature, humidity, and the corresponding ECG sample, and forward it to the platform. Six seconds record at 970Sa/s corresponding to 5820, the system shuts down automatically.

The MQTT broker is the central point of communication, and it is in charge of dispatching all messages between the senders and the rightful receivers. A client is any device that connects to the broker and can publish or subscribe to topics to access the information. A topic contains the routing information for the broker. Each client that wants to send messages publishes them to a certain topic, and each client that wants to receive messages subscribes to a certain topic. The broker delivers all messages with the matching topic to the appropriate clients

3 User Query Intent and Storage of Tags

This section is actually divided in two main sub-sections the first part is all about putting all the hardware together with few adjustments, the second part is all about programming the ESP8622 in Lua language, and Android programing.

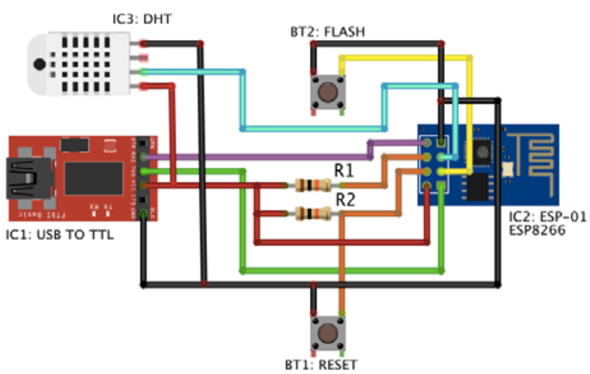

a
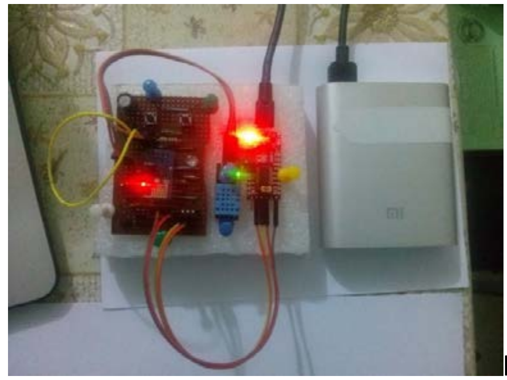
b

Figure 6: a) System Implementation b)Components setup for Data transmission using ESP8266-01

The system takes advantage of the HTTP (HyperText Transfer Protocol) protocol, to send a web page to any client requesting that page, from any web browser, or any request converted from android applications to http request, providing that his device is attached to the distributor's network, as shown in **Error! Reference source not found.**. This architecture can easily run an HTTP server, accessible through its station mode, and connected to an access point. The core component is a Microcontroller unit based NodeMcu: ESP8266-12E WIFI module,

Figure 7: Chart visualisation for Temperature, Humidity, ECG, dataset plot through MatLab

4 Discusion

From the Figure 7 Field 3 the relative Humidity, associated with the patient's room ambient Temperature, in Field2. These parameters were obtained with a DHT11 coupled to the NodeMCU, then pushed to the IoT platform ThingSpeak between 08h and 11h. The associated ECG is presented on the Field 4 where we can distinguish PQRS waves sent in alongside with temperature and the humidity. The plot 6 presents a set of data transferred from 07h55 to 10h30, and displayed through IoT with the use of MatLab for further processing. This could also be joined Tchamda et al [25] developed to obtain a mini health station. With regards with the work done by Hangsik Shin [15], this work could be considered as implement supplemented with IoT. As compare to [4] our contribution stands as a hardware add-on, for that architecture.

5 Conclusion

The advent of IoT coupled to telemedicine has enhanced use telecommunication tools, within the framework of clinical health, to carefully diagnose diseases remotely. We made use of low cost and open source tools to accurately transmit patient’s parameters to an IoT platform. Our contribution carried on transmitting ECG samples, concatenated with temperature and humidity as additional parameters. The transmission was made possible by connecting to the NodeMCU to ThingSpeaktm which is one of the most advanced IoT platform embedding MatLab. We made use the MQTT and REST Application Program Interface. As result of that experimentation we succefully pushed those three parameters, necessary on heart disease diagnosis. The main limitation of such architecture is the authorize time between two data push which is ten seconds, making it slow when acquiring parameters. This setup will be of a great help for remote medical data processing, because the IoT platform selected gave room to MatLab for further processing. The next phase for this work is a dedicated IoT platform to enhance, to overcome those limitations.

REFERENCES

[1] J. Grigsby, "Telemedicine in the United States," Telemedicine: Theory and practice, p. 291–325, 1997.

[2] Wikipedia, "Telemedicine," 2017. [Online]. Available: https://en.wikipedia.org/wiki/Telemedicine#cite_note-1. [Accessed 20 May 2017].

[3] W. PAMELA and D. S. BEVERLY, "Evolution of Telemedicine from an Applied Communication Perspective in the United States," TELEMEDICINE AND e-HEALTH, vol. 12, no. 05, 2006.

[4] T. Tchapga, D. Tchiotsop, E. M. Sone, G. Tchimmoue, E. Abuno and A. Fomethe, "ECG Acquisition Based AVR Microcontroller and Java Application for Visualisation via Email Service," International Journal of Advanced Research in Computer Science and Software Engineering, vol. 7, no. 1, pp. 153-158, 1 2017.

[5] Tamas H., "Wireless ECG/EEG with the MSP430 Microcontroller," pp. 20-50, 2009.

[6] R. Amir-Mohammad, N. Pekka, L. Pasi and T. Hannu, "Towards Energy-Efficient HealthCare: an Internet-of-Things Architecture Using Intelligent Gateways," in International Conference on Wireless Mobile Communication and Healthcare, 2014.

[7] K. Sung-Yuan, W. Kang-Min, L. Wei-Cheng and K. Chun-Heng, "A Portable ECG Recorder," in Consumer Electronics, Communications and Networks (CECNet), 21-23 April 2012.

[8] V. Saurabh Prakash, "Real time monitoring of ECG signal using PIC and web server," International Journal of Engineering and Technology (IJET), vol. 5, no. 2, pp. 1047-1053, Apr-May 2013.

[9] G. TCHIMMOUE, J. KAMDEM and A. S. NKO'O, "Didacticiel d'Instrumentation Virtuel à Coût Réduit pour l'Acquisition et le Traitement des Signaux ECG," EDP Sciences, Vols. 11,2012, no. 0002, p. 16, 2012.

[10] D. TCHIOTSOP, T. KANA, M. FOGUE, N. A. ,. TCHOUANI and K. KENTSA, "Low Cost and Low Power ECG Recorder Suitable for Low Incomes Populations," International Journal of Electronics Communication and Computer Engineering, vol. 6, no. 5, pp. 558-564, 2015.

[11] D. Tchiotsop, T. Kanaa, M. Fogué, N. L. Nguemkoua, P. Mongoue and M. I. Toumtap, "ASCII Encoding of Biomedical Signals for SMS Transmission," International Journal of Electronics Communication and Computer Engineering, vol. 6, no. 3, pp. 409-415, 2014.

[12] Purnima, R. Neetu, T. Rahul and B. Renuka, "ZIGBEE AND GSM BASED PATIENT HEALTH MONITORING SYSTEM," International Journal of Advanced Research in Electrical, Electronics and Instrumentation Engineering, vol. 3, no. 1, pp. 6664-6669, January 2014.

[13] W. Ying-Chieh, W. Ying-Yu, C. Kai-Hsiung and L.-S. Jang, "DESIGN OF A MICROCONTROLLER-BASED REAL-TIME HEART RATE VARIABILITY MEASUREMENT SYSTEM USING A LOW-COMPLEXITY R-PEAK DETECTION ALGORITHM," Instrumentation Science & Technology, vol. 41, no. 3, pp. 274-289, 2013.

[14] T. M. Lionel and K. P. E. Martin, "Universal Module of Acquisition and Transmission of Electrophysiological Signal," International Journal of Innovative Research in Science, Engineering and Technology, vol. 3, no. 6, pp. 13767-13776, 2014.

[15] S. Hangsik, "Ambient temperature effect on pulse rate variability as an alternative to heart rate variability in young adult," Journal of Clinical Monitoring and Computing, vol. 30, no. 06, p. 939–948, 2015.

[16] E. Opher, F. Fabiana and A. Sarit, "Tutorial on the Internet of Everything," in 8th ACM Int. Conf. on Dist. Event-Based Sys., Munbai/India, 2014.

[17] S. Hyejeong and G. Ranjit, "Digitally intensive transmitter employing RF pulse width modulation for IoT applications," in Radio Frequency Integrated Circuits Symposium (RFIC), 2015 IEEE, 17-19 May 2015.

[18] Rahmani, N. K. Thanigaivelan, T. N. Gia, J. Granados, B. Negash, P. Liljeberg and H. Tenhunen, "Smart e-health gateway: bringing intelligence to internet-of-things based ubiquitous healthcare systems," 2016.

[19] S. Andrej, K. Andrej, K. Davorin, R. Stojanovic, S. Vladimir, Eugene and k. Semen, "Streaming Pulse Data to the Cloud with Bluetooth LE or NODEMCU ESP8266," in 5th Mediterranean Conference on Embedded Computing, Bar, Montenegro, 2015.

[20] J. K. B and V. K, "Energy Efficient Lightening System for an Indoor Environment using Wireless Sensor Network Based on IOT," International Journal of Research and Scientific Innovation, vol. 3, no. 5, pp. 144-148, May 2016.

[21] K. P. Krupal, P. Jignesh and P. Hitesh, "Low Cost Home Automation with ESP8266 and Lightweight protocol MQTT," Transactions on Engineering and Sciences, vol. 3, no. 6, December 2015.

[22] C. G and R. H, "IOT Controlled Two Wheel Self Supporting Robot Without External Sensor," Middle-East Journal of Scientific Research, pp. 286-290, 2015.

[23] Purnima, R. Neetu, T. Rahul and B. Renuka, "ZIGBEE AND GSM BASED PATIENT HEALTH MONITORING SYSTEM," International Journal of Advanced Research in Electrical, Electronics and Instrumentation Engineering, vol. 3, no. 1, 2014.

[24] D. Arko and W. Michael, "Ambient Environmental Quality Monitoring Using IoT Sensor Network," INTERNETWORKING INDONESIA JOURNAL, vol. 8, no. 1, 2016. R. Tchamda, T. R, B. P. Francois and K. M, "Monitoring System of Mechanical Activity of the Heart and Goelocalization of the Patient Based on the Mqtt Cloud," vol. 4, no. 5, pp. 1-8, 2017.

[25] MathWorks, "Choose Between REST API and MQTT API," MathWorks, [Online]. Available: https://www.mathworks.com/help/thingspeak/choose-between-rest-and-mqtt.html?requestedDomain=true. [Accessed 12 December 2017].

Society for Science and Education United Kingdom

JBEMI JOURNAL OF BIOMEDICAL ENGINEERING AND MEDICAL IMAGING

ISSN: 2055-1266
Volume 5 Issue 3

Diagnosis of Brain Lesions, Glioma, Multiple-Sclerosis and Metastases from MRI: An efficient classifier-aided method using Refractive Index as a surrogate Biological Marker

Sparsh Jain, [1,2]Tapan K Biswas, [1]Rajib Bandyopadhyay

[1]*Department of Instrumentation and Electronics Engineering, Jadavpur University, Kolkata, India;*
[2]*(Former) Harvard University, Brigham and Women's Hospital, Boston MA, United States of America;*
sparshju@gmail.com; tbiswas52@gmail.com; rb@iee.jusl.ac.in

ABSTRACT

We introduce a highly accurate method of diagnosing the various pathological conditions that might exist in a subject's brain, like edema, multiple sclerosis (Tumefactive, Relapsing-remitting, secondary-progressive, primary-progressive and progressive-relapsing), glioma, glioblastoma and metastases. These show up on conventional MRI scans, but it is often difficult to identify the exact type of the pathology from the grayscale image. We employ the use of Support Vector Machines (SVM) to work on the MR Spectroscopy [6, 12] data and correctly identify the condition-especially in seemingly vague cases where radiologists cannot rule out high uncertainty in their conclusion. The SVM trains on data sets collected for different patients and optimizes its hyperplanes based on eight input variables – T2, CHO, ADC, CR, CHO/NAA, CR/NAA, LIP/LAC, MI, CH/CR, T2 periphery [6] and Refractive index. Refractive index is an additional parameter which we include to get better boundary lines and accuracy, as shown in our prior works [10]. We test this SVM on a set of 19 patients' data and achieve 100% accuracy in predictions. The training and testing is carried out in MATLAB.

Keywords: Magnetic Resonance Imaging, MR Spectroscopy, Refractive Index, Support Vector Machine (SVM), Brain Lesions, Cancer.

1 Introduction

Only structural changes of MR images of aneurysms, Glioma or other brain tumours including metastasis or secondary deposits of cancer tissues cannot be sufficient for accurate diagnosis [1]. Data collected from metabolites of MR spectroscopy like NAA, Choline, Creatine, lipid or lactate or physical data like Refractive Indices (RI), T2 magnetic relaxation values, and Apparent Diffusion Coefficient (ADC) values are also important for correct diagnosis of the disease. Figures 1 to 4 show how a few of these diseases appear on the scans [Fig 1-4].

If the supporting data are available, live prediction of diseases or of the tissue can be performed with 90 to 95% accuracy using Support Vector Machines (SVM). Clustering of diseases and tissues can also be done using SVMs. It is worth mentioning that machine learning tools like clustering, SVM and neural

DOI: 10.14738/jbemi.53.4700
Publication Date: 19th June 2018
URL: http://dx.doi.org/10.14738/jbemi. 53.4700

networks (Principal Component Analysis) have previously been used for similar purposes on MRI data [5, 10, 13-15].

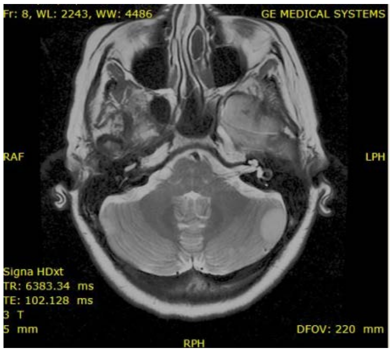

Figure 1: Metastasis MRI

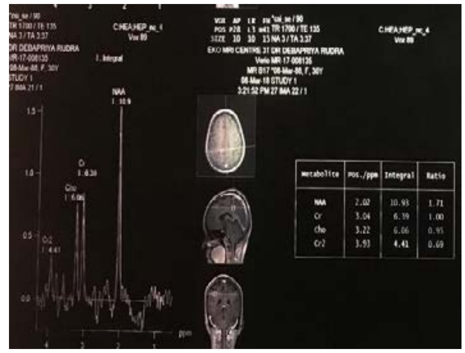

Figure 2: MR Spectroscopy (MRS) Normal

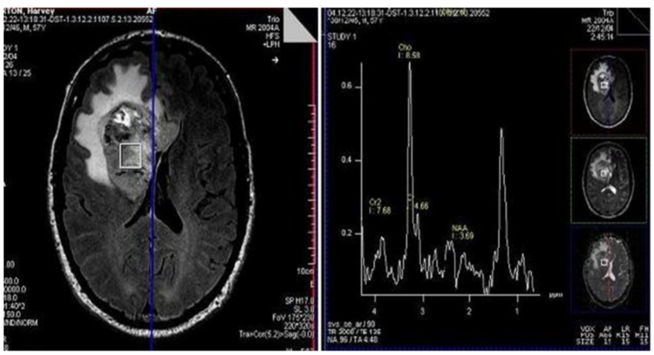

Figure 3: Grade-3 Glioblastoma with abnormal MRS

Figure 4: Multiple Sclerosis (MS) MRI

2 Background

SVM employs a nonlinear classification method [2]. It is implemented to assess and make virtual pathological predictions using the data obtained from MRI, various metabolic components and their ratio of MR Spectroscopy, ADC, RI and T2 values (Table 1).

An SVM with extraordinary data processing uniqueness, nonlinearity and learning with generalization capability is used to characterize the disease. Thus there are 10 independent numeric variables. SVM and Neural Network (NN) both belong to supervised learning methods, but their working procedure is different.

We have used Error correcting output codes (ECOC) mode to reduce the errors in classification. ECOC is an error-correcting output codes classifier used to get multiclass learning by diminishing multiple binary classifiers for instance SVMs [3].

The main factor responsible for the performance of ECOC methods is the self-determination of binary classifiers, otherwise the ECOC method will be unsuccessful. It is effective in multiple classes and requires a coding design. This design determines the classes. Binary learners undergo training and a decoding system determines the prediction of the binary classes.

a) The coding design is one-versus-one.

b) Decoding procedure would utilize loss *g*.

c) SVMs will be the learners.

SVM utilizes a function or hyperplane [4] among different classes giving a maximum margin parameter. This hyperplane tries to divide the classes so that each groups remains on either side of the plane and by a particular boundary. Our SVM handles 10 variables. It has 8 output results or classes of different types of tissue (such as CSF, gray matter, white matter) and diseases like low and high grade glioma and metastasis for targeted prediction.

Improved classification accuracy can be achieved by ECOC models compared to other multiclass model.

3 Method

The data has been used from the authors' prior research [5] (Table1). We train the SVM using data from 116 patients. The SVM is then tested on data from 19 patients.

The method consists of two parts:

a) Training the SVM using available data

b) Testing the trained SVM to classify unknown data.

3.1 Source Code and Platform

The SVM training and classification work has been implemented on the 64-bit MATLAB R2017a environment on Windows 10 Home platform. Access to the source code and complete training data can be requested by contacting the corresponding author.

3.2 Training the Support Vector Machine

3.2.1 3.2.1 Identification

First we identify the label and data. Label includes the names of tissue or diseases like MS, Glioma etc. Data corresponds to all the numerical values associated with each label. SVM essentially matches the data sets with the correct labels. The first column of Table 1 has all the labels. The remaining 11 columns contain the data. So for example, row no. 5 has the label CSF and that particular CSF scan has 11 values corresponding to T2, ADC, CR, CHO etc [6].

Keys for tables 1-4:

'CSF': Cerebrospinal fluid

'gmatter': Gray Matter

'gblastma': Glioblastoma

'MS': Multiple sclerosis

'w matter': White Matter

'mets': Metastases

Table 1: Preview of the entire data set. 41 out of 135 sets are shown below.

TISSUE	T2	CHO	ADC	CR	CHO/NAA	CR/NAA	LIP/LAC	MI	CH/CR	T2peri	RI
CSF	400	1610	300	1400	0.402	0.346	1400	910	1.15	400	1.3333
CSF	399	1676	307	1450	0.404	0.347	1489	917	1.15	399	1.3333
CSF	398	1689	311	1560	0.408	0.351	1550	957	1.15	399	1.3333
CSF	397	1700	313	1600	0.409	0.357	1554	987	1.15	399	1.3333
CSF	396	1728	320	1788	0.412	0.361	1660	1050	1.14	395	1.3333
CSF	395	1711	322	1800	0.422	0.367	1701	1056	1.14	395	1.3333
CSF	394	1710	322	1809	0.423	0.368	1690	1059	1.14	394	1.3333
CSF	345	2021	402	2060	0.572	0.448	1744	1145	1.15	345	1.3333
CSF	344	2022	403	2061	0.573	0.451	1744	1145	1.15	344	1.3333
CSF	343	2023	404	2062	0.574	0.452	1745	1146	1.15	343	1.3333
CSF	342	2024	405	2068	0.577	0.453	1746	1147	1.15	342	1.3333
CSF	341	2123	411	2063	0.578	0.453	1747	1148	1.15	341	1.3333
ms	340	11750	145	8320	0.779	0.557	4160	2912	1.4	340	1.3334
ms	339	11750	1460	8319	0.778	0.541	4423	3223	1.4	339	1.3335
ms	338	11749	1459	8314	0.776	0.538	4423	3221	1.4	338	1.3336
ms	337	11746	1445	8311	0.774	0.536	4421	3220	1.4	337	1.3421
ms	336	11745	1444	8310	0.773	0.534	4422	3219	1.4	336	1.3439
ms	335	11745	1443	8309	0.772	0.532	4420	3216	1.4	335	1.3498
ms	334	11743	1443	8308	0.771	0.531	4419	3214	1.4	334	1.3499
ms	304	5947	120	5400	0.873	0.7396	6766	4294	1.1	245	1.3519
ms	249	3448	112	3320	0.821	0.7112	5423	2322	1.02	230	1.3589
ms	245	1610	110	2212	0.465	0.941	1440	2276	0.495	227	1.3641
gmatter	130	1601	72	2209	0.464	0.938	1439	361	0.491	166	1.3956
gmatter	129	1599	73	2208	0.463	0.936	1437	357	0.4911	165	1.3956
gmatter	128	1597	74	2206	0.463	0.934	1435	351	0.489	165	1.3956
w matter	95	1180	70	2443	0.453	0.788	1345	312	0.488	148	1.4251
w matter	93	1108	71	2435	0.447	0.771	1341	320	0.468	146	1.4256
w matter	93	1067	89	2301	0.444	0.775	1167	324	0.466	169	1.4262
edema	160	1231	132	2216	0.443	0.776	1123	325	0.467	246	1.3741
edema	182	1331	130	2321	0.442	0.787	1011	321	0.456	243	1.3823
edema	191	1451	131	2356	0.441	0.778	990	313	0.445	245	1.3822
edema	193	1452	130	2340	0.441	0.768	990	312	0.445	245	1.3823
GLIOMA	90	1443	127	2243	0.431	0.766	989	310	0.423	175	1.4331
GLIOMA	99	1365	177	2254	0.341	0.712	917	300	0.343	170	1.4339
GLIOMA	107	2213	155	2114	0.333	0.677	901	310	0.321	191	1.4456
Gblastma	108	2457	154	2115	0.332	0.676	900	311	0.311	195	1.4512
Gblastma	109	2655	152	2112	0.332	0.676	900	311	0.311	195	1.4539
Gblastma	128	1284	131	2589	0.541	0.781	1767	322	0.76651	198	1.4723
METS	129	1298	130	2567	0.511	0.657	1011	323	0.432	200	1.4831
METS	130	1301	130	2478	0.511	0.657	1011	323	0.432	200	1.4831
METS	152	1412	132	2022	0.425	0.713	1121	357	0.451	224	1.4913

3.2.2 Training

We use the Fitcecoc command in Matlab to train an SVM for the data and label we already have (Table 2). SVM uses Supervised Learning and classifies data. The basic command for SVM training is FitSVM or svmtrain but that can be used only for binary classification i.e. when there are only two classes/labels [7]. In this case we have 8 different labels, so we use fitcecoc, which can accommodate multiple classes. SVM and Neural networks both work on supervised learning but their mechanisms differ.

So the output variable generated is the Support Vector Machine trained using the data.

Table 2: Preview of the Training data set. 16 out of 116 sets are shown below.

TISSUE	T2	CHO	ADC	CR	CHO/NAA	CR/NAA	LIP/LAC	MI	CH/CR	T2peri	RI
CSF	400	1610	300	1400	0.402	0.346	1400	910	1.15	400	1.3333
CSF	398	1689	311	1560	0.408	0.351	1550	957	1.15	399	1.3333
CSF	394	1710	322	1809	0.423	0.368	1690	1059	1.14	394	1.3333
ms	340	11750	145	8320	0.779	0.557	4160	2912	1.4	340	1.3334
ms	336	11745	1444	8310	0.773	0.534	4422	3219	1.4	336	1.3439
ms	245	1610	110	2212	0.465	0.941	1440	2276	0.495	227	1.3641
gmatter	130	1601	72	2209	0.464	0.938	1439	361	0.491	166	1.3956
gmatter	128	1597	74	2206	0.463	0.934	1435	351	0.489	165	1.3956
w matter	95	1180	70	2443	0.453	0.788	1345	312	0.488	148	1.4251
edema	160	1231	132	2216	0.443	0.776	1123	325	0.467	246	1.3741
edema	193	1452	130	2340	0.441	0.768	990	312	0.445	245	1.3823
GLIOMA	90	1443	127	2243	0.431	0.766	989	310	0.423	175	1.4331
Gblastma	108	2457	154	2115	0.332	0.676	900	311	0.311	195	1.4512
Gblastma	128	1284	131	2589	0.541	0.781	1767	322	0.76651	198	1.4723
METS	130	1301	130	2478	0.511	0.657	1011	323	0.432	200	1.4831
METS	152	1412	132	2022	0.425	0.713	1121	357	0.451	224	1.4913

3.3 Testing the SVM to predict the classes of unknown data sets

Using a few data sets (which were not used to train the SVM) we test the SVM. The data (Table 3) to the SVM is fed and it predicts the classes on its own.

Table 3: Test data set. The trained SVM predicts the classes for 19 unknown data sets.

TISSUE	T2	CHO	ADC	CR	CHO/NAA	CR/NAA	LIP/LAC	MI	CH/CR	T2peri	RI
CSF	400	1610	300	1400	0.402	0.346	1400	910	1.15	400	1.3333
CSF	399	1676	307	1450	0.404	0.347	1489	917	1.15	399	1.3333
CSF	398	1689	311	1560	0.408	0.351	1550	957	1.15	399	1.3333
CSF	395	1711	322	1800	0.422	0.367	1701	1056	1.14	395	1.3333
CSF	394	1710	322	1809	0.423	0.368	1690	1059	1.14	394	1.3333
ms	337	11746	1445	8311	0.774	0.536	4421	3220	1.4	337	1.3421
ms	335	11745	1443	8309	0.772	0.532	4420	3216	1.4	335	1.3498
ms	334	11743	1443	8308	0.771	0.531	4419	3214	1.4	334	1.3499
ms	304	5947	120	5400	0.873	0.7396	6766	4294	1.1	245	1.3519

gmatter	128	1597	74	2206	0.463	0.934	1435	351	0.489	165	1.3956
w matter	95	1180	70	2443	0.453	0.788	1345	312	0.488	148	1.4251
w matter	93	1067	89	2301	0.444	0.775	1167	324	0.466	169	1.4262
edema	191	1451	131	2356	0.441	0.778	990	313	0.445	245	1.3822
edema	193	1452	130	2340	0.441	0.768	990	312	0.445	245	1.3823
GLIOMA	90	1443	127	2243	0.431	0.766	989	310	0.423	175	1.4331
GLIOMA	107	2213	155	2114	0.333	0.677	901	310	0.321	191	1.4456
Gblastma	108	2457	154	2115	0.332	0.676	900	311	0.311	195	1.4512
METS	129	1298	130	2567	0.511	0.657	1011	323	0.432	200	1.4831
METS	152	1412	132	2022	0.425	0.713	1121	357	0.451	224	1.4913

4 Results

We ran our trained SVM on a data set of 19 patients. These 19 sets were excluded from the training set for obvious reasons. We had the original diagnoses prior to running the code. The SVM successfully classified each of the 19 data sets accurately. No misclassification was encountered. We retrained the SVM by taking different data sets out of the training set and using them for test purposes, owing to lack of new data. Multiple tests yielded consistently accurate results i.e. the SVM perfectly classified the data with 0% uncertainty or false classifications. Thus, this Support Vector Machine enabled code correctly diagnoses the seven different types of brain diseases reliably. It also clearly differentiates between normal CSF tissue and lesions/pathological conditions.

Results are recorded in Table 4.

Table 4: Final results comparing the SVM prediction to the actual diagnoses.

ORIGINAL PATIENT DIAGNOSIS	RESULT PREDICTED BY OUR SVM	ACCURACY OF PREDICTION
'CSF'	'CSF'	Accurate Classification
'CSF'	'CSF'	Accurate Classification
'ms'	'ms'	Accurate Classification
'ms'	'ms'	Accurate Classification
'gmatter'	'gmatter'	Accurate Classification
'gmatter'	'gmatter'	Accurate Classification
'w matter'	'w matter'	Accurate Classification
'w matter'	'w matter'	Accurate Classification
'edema'	'edema'	Accurate Classification
'edema'	'edema'	Accurate Classification
'GLIOMA'	'GLIOMA'	Accurate Classification
'GLIOMA'	'GLIOMA'	Accurate Classification
'Gblastma'	'Gblastma'	Accurate Classification
'Gblastma'	'Gblastma'	Accurate Classification
'Gblastma'	'Gblastma'	Accurate Classification
'METS'	'METS'	Accurate Classification
'METS'	'METS'	Accurate Classification
'METS'	'METS'	Accurate Classification
'METS'	'METS'	Accurate Classification

5 Conclusion

It can be concluded that the use of Support Vector Machines and other tools of Machine Learning [8] can be employed to achieve extremely reliable and accurate diagnostic results in cases where conventional imaging techniques offer less clarity, and where biopsies [9] carry potential risks to the patient. An added advantage of using SVM for this purpose is that it guarantees reproducibility and repeatability i.e. the accuracy levels are guaranteed to remain fairly constant over multiple runs and long periods of time. Along with the custom-developed colour palette [10] using refractive index, it also provides a much sharper contrast image of the brain. We here note that the accuracy is limited only by the size of the data set we use for training the SVM initially. Owing to our present setup, we are unable to record new data on a rolling basis. A further step towards making it more reliable and robust would include obtaining new data in large amounts, and incorporating these data points into the training set. Different classification algorithms can further be integrated with this to achieve even better and conclusive results in all cases. It is safe to declare that Support Vector Machines will find their use in day-to-day radiological and imaging methods for common use due to their superior accuracy, fail-proof safety fallbacks and evolving classification algorithms. This in turn will slowly reduce the need to perform invasive biopsies and multiple tests, as well as make diagnoses less dependent on the human radiologist/ practitioner who might be prone to making errors [11].

REFERENCES

[1] Schwab, K.E., Gailloud P, Wyse G, Tamargo R.J., *Limitations of magnetic resonance imaging and magnetic resonance angiography in the diagnosis of intracranial aneurysms*. *Neurosurgery*, Volume 63, Issue 1, 1 July 2008

[2] Support Vector Machines - http://www.statsoft.com/Textbook/Support-Vector-Machines

[3] Mingxia Liu, Daoqiang Zhang, *Joint Binary Classifier Learning for ECOC-Based Multi-Class Classification*. IEEE Transactions on Pattern Analysis and Machine Intelligence (Volume: 38, Issue: 11, Nov. 1 2016)

[4] Pardalos P.M. (2008) *Hyperplane Arrangements in Optimization*. In: Floudas C., Pardalos P. (eds) Encyclopedia of Optimization. Springer, Boston, MA

[5] Tapan K Biswas, R Bandyopadhyay, A Dutta, *Validating The Discriminating Efficacy Of MR T2 Relaxation Value Of Different Brain Lesions And Comparison With Other Differentiating Factors: Use Of Artificial Neural Network And Principal Component Analysis*. The Internet Journal of Radiology (Volume 20, No. 1)

[6] Radiopedia Introduction to MR Spectroscopy, https://radiopaedia.org/articles/mr-spectroscopy-1.

[7] Mathworks Guide, Support Vector Machines for Binary Classification.

[8] Machine Learning, Wikipedia, https://en.wikipedia.org/wiki/Machine_learning.

[9] Nor M., Noor Rahman, J. Adnan, *Intracranial Bleed Post Stereotactic Biopsy: Lessons Learned*, The Internet Journal of Neurosurgery (Volume 8, Number 1)

[10] Tapan K Biswas, S R Choudhury, A Ganguly, R Bandyopadhyay, A Dutta, *Refractive Index As Surrogate Biological Marker Of Tumefactive And Other Form Of Multiple Sclerosis And Its Superiority Over Other Methods*. The Internet Journal of Radiology (Volume 19, Number 1).

[11] Blake A. Johnson, *Avoiding diagnostic pitfalls in neuroimaging.* Applied Radiology-The Journal of Practical Medical Imaging and Management 2016;45(3):24-29. March 02, 2016

[12] Wikipedia, Nuclear Magnetic Resonance Spectroscopy, https://en.wikipedia.org/wiki/Nuclear_magnetic_resonance_spectroscopy

[13] Kasai, M., Yasuda, Y., Mizoguchi, H., Soga, K., Kaneko, K., & Takemura, H. (2017). *In vivo tumor wavelength band selection using Hierarchical clustering and PCA with NIR-Hyperspectral Data*. Journal of Biomedical Engineering and Medical Imaging, *4*(1), 01.

[14] Limam, O. (2016). *MRI Segmentation based on Multiobjective Fuzzy Clustering*. Journal of Biomedical Engineering and Medical Imaging, *3*(2), 07.

[15] Abd El kader, I., Zhang, S., & Xu, G. (2017). *Improved Fuzzy C-Means Algorithm for Brain Tumor Identification Analysis Using Magnetic Resonance Brain Images*. Journal of Biomedical Engineering and Medical Imaging, 4(3), 15.

Society for Science and Education United Kingdom

JBEMI Journal of Biomedical Engineering and Medical Imaging

ISSN: 2055-1266
Volume 5 Issue 3

Effect of Anthropogenic Activities on Surface and Ground Water in Ogwuama Community of Ahiazu, IMO State, Nigeria

Tochukwu Ezechi Ebe[1], Roseline Feechi Njoku-Tony[2], Ihejirika C. E.[3], Emereibeole E[4]. I., Nicholas Chima Ndukwu[5], Mgbemena I. C.[6] And Augusta Anuli Nwachukwu[7]

[1, 2, 3, 4 and 5]Department of Environmental Technology, School of Environmental Sciences, Federal University of Technology, Imo State, Nigeria.

[6 and 7]Department Of Biotechnology, School Of Biological Sciences, Federal University Of Technology,Imo State, Nigeria.

akumziri@gmail.com

ABSTRACT

Human activities have become a major source of environmental pollution especially on the issue of water pollution which includes surface and ground water. This research was aimed at studying the effect of human activities such as indiscriminate defecation, fermentation of cassava tubers etc on the water quality of Onuakpaka stream and selected ground water in Ogwuama community of Ahiazu, Imo State, Nigeria. Water samples were collected in triplicates each with sterile containers from upstream, downstream and ground water. All the samples were analyzed using standard method. The result showed that the pH of samples collected from the upstream and downstream were more acidic (5.70 and 5.90 respectively) than the ground water (6.06). Also, the upstream and downstream have high turbidity of 14.76 and 15.40 respectively. More also, dissolved oxygen in the stream samples were below the World Health Organization and Federal Ministry of Environment standards while the ground water samples were within the standard. Also there were presence of feacal counts and *Escherichia coli* in all the samples collected (8.00 in ground water, 13.00 in the upstream and 23.00 downstream) this may be due to indiscriminate defecation. Furthermore, the temperature, conductivity, total dissolved oxygen etc were within the standard in all the samples collected. Conclusively, the presence of feacal contaminant and *Escherichia coli* signifies that the water is highly polluted and unfit for drinking and domestic work. This posses a great danger to human health in this community.

Keywords: contamination, anthropogenic, upstream, downstream, ground water.

1 Introduction

Water is very important in our day to day activities. Sources of water in Ogwuama community are stream and ground water. Water is a scarce and fading resource and its management can have an impact on the flow and the biological quality of rivers and streams. The quality of water source is influenced majorly by anthropogenic activities. Such as cassava fermentation and intensive agricultural practice, washing of cloths, bathing, defecation and discharge of massive amount of waste around the

DOI: 10.14738/jbemi.53.4542
Publication Date: 20th June 2018
URL: http://dx.doi.org/10.14738/jbemi. 53.4542

water source. The impact of these anthropgenic activities has been so extensive that the water bodies have lost their significant capacity to a large extent.

The quality of water is determined by monitoring microbial load especially feacal coliform and physico-chemical parameters like pH, Dissolved oxygen, Biochemical oxygen demand etc. The problem of ground water contamination include outbreaks of water-borne diseases , as well as unsuitability of water for both agricultural and domestic uses. Low water tables may cause low infiltration rates.

2 Materials and Method

2.1 Study Area

Ogwuama in Ahiazu Mbaise, Imo State of Nigeria is located within 7° 14′ 348′′ to 7° 18′ 44′′ E and 5° 31′ 006′′ to 5° 35′ 56′′ N. The climate of the area is humid tropical and typifies the rain forest zone of the equatorial region. Mean ambient temperature is 28^0C. Wet season last between April to November with a short dry season lasting the rest of year.

2.2 Sample Collection

Water samples were randomly collected from Onuakpaka stream using 500ml sterile containers at three different points on the upstream and downstream and from three different public groundwater using standard method.

2.3 2.3 Determination of Physico-Chemical Parameters

The pH, temperature, conductivity, total dissolved solid and dissolved oxygen were determined in-situ using jenway(Hanna 1910) multipurpose tester in each sampling point while the BOD was determined using a winkler method for a period of five days at 20^0C.

Also, the turbidity was determined by photometric method using HACH DR/2010 spectrometer at a wavelength of 860nm.

More also, Argentometric method described by APHA (2005) was used to determine the chloride content.

EDTA titrimetric method was used to determine total hardness.

Nitrate was determine by cadmium reduction method using H183200 multiparameter bench photometer at a wavelength of 525nm.

2.4 Microbial Analysis of Samples

Samples were serially diluted and aliquots of 0.1ml of each water sample was used to inoculated on plate, Eosin methylene blue agar and potato dextrose agar nutrient were added by spread plate method. These plates were then incubated at 37°C for 24hrs for bacteria Colonies and 25°C, 78hrs–120hrs for fungi Colonies. After incubation, colonies were identified, counted and recorded.

3 Results and Discussion

3.1 Results

A total of 9 samples were collected (three samples each from the upstream, downstream and ground water).

Table 1: The physico-chemical and microbial analysis results of well water.

Parameter	FMEMV Standard	WHO Standard (2008)	Ground water 1	Ground water 2	Ground water 3	Mean value
pH	6.5 – 8.5	6.5 – 9.5	6.06	6.07	6.05	6.06
Temp (ºC)	20 – 30	N/A	26	28	27	27
Conductivity (Us/cm)	100	100	109	111	107	109
Turbidity (NTU)	10	5	0.00	0.00	0.00	0.00
DO (mg/l)	>4	4	4.18	4.20	4.22	4.20
BOD (Mg/l)	10	6	1.8	2.1	2.1	2.0
Total Dissolved solid(mg/l)	250	250	70.87	70.85	70.83	70.85
Total Chloride(mg/l)	250	250	-	145.08	145.10	145.08
Total Hardness(mg/l)	200	200	145.06	2.1	2.4	2.3
Nitrate(mg/l)	40	45	22.88	22.93	22.89	22.90
Total faecal count (cfu)	0	N/A	9	11	10	10
Total E-Coli Count(cfu)	0	N/A	9	9	6	8

N/A = Not Available

Table 2: The physico-chemical and microbial analysis results of Upstream.

Parameter	FMEMV Standard	WHO Standard (2008)	Upstream 1	Upstream 2	Upstream 3	Mean value
pH	6.5 - 8.5	6.5 – 9.5	5.71	6.69	5.70	5.70
Temp (°C)	20 – 30	N/A	27	27	27.3	27.1
Conductivity (Us/cm)	100	100	8	10	12	10
Turbidity (NTU)	10	5	14.65	14.30	15.33	14.76
DO (mg/l)	>4	4	3.57	3.55	3.68	3.60
BOD (Mg/l)	10	6	2.4	2.0	1.99	2.1
Total Dissolved solid(mg/l)	250	250	6.00	6.40	7.10	6.50
Total Chloride(mg/l)	250	250	65.9	70.0	82.81	72.9
Total Hardness(mg/l)	200	200	0.5	0.6	0.7	0.6
Nitrate(mg/l)	40	45	10.97	10.90	10.83	10.90
Total faecal count (cfu)	0	N/A	22	22	22	22
Total E-Coli Count(cfu)	0	N/A	9	12	18	13

N/A=Not Available

Table 3: The physico-chemical and microbial analysis results of downstream.

Parameter	FMEMV Standard	WHO Standard (2008)	Down-stream 1	Down-stream 2	Down-stream 3	Mean value
pH	6.5 - 8.5	6.5 – 9.5	5.80	5.90	6.00	5.90
Temp (°C)	20 – 30	N/A	27.1	27.3	27.5	27.3
Conductivity (Us/cm)	100	100	11	11	14	12
Turbidity (NTU)	10	5	15.48	15.60	16.14	15.74
DO (mg/l)	>4	4	3.57	3.80	3.85	3.80
BOD (Mg/l)	10	6	0.79	0.70	0.61	0.70
Total Dissolved solid(mg/l)	250	250	7.10	7.60	8.70	7.80
Total Chloride(mg/l)	250	250	150	172.6	224	182.2
Total Hardness(mg/l)	200	200	0.65	0.70	0.75	0.70
Nitrate(mg/l)	40	45	0.36	0.28	0.26	0.30
Total faecal count (cfu)	0	N/A	28	40	52	40
Total E-Coli Count(cfu)	0	N/A	20	22	27	23

N/A=Not Available

Table 4: The mean standard deviation of the water samples

Parameters	FMENV Std	Well water	Up stream	Down stream
pH	6.5-8.5	6.06±0.01	5.70±0.01	5.90±0.10
Temp (^{o}C)	20-30	27.00±1.00 [a]	27.10±0.17 [a]	27.30±0.20 [a]
Conductivity (Us/cm)	100	109.00±2.00[b]	10.00±2.00 [b]	12.00±1.73 [b]
Turbidity (NTU)	10	0.00±0.00	14.76±0.52	15.74±0.35
DO (mg/l)	>4	4.20±0.02	3.60±0.07	3.80±0.05
BOD (Mg/l)	10	2.00±0.17	2.13±0.23	0.70±0.09
Total Dissolved solid(mg/l)	250	70.85±0.02[c]	6.50±0.56 [c]	7.80±0.82 [c]
Total Chloride(mg/l)	250	145.08±0.02[d]	72.90±8.82 [d]	182.20±3.02 [d]
Total Hardness(mg/l)	200	2.30±0.17	0.60±0.10	0.70±0.05
Nitrate(mg/l)	40	22.90±0.03[e]	10.90±0.07 [e]	0.30±0.05 [e]
Total faecal count (cfu)	0	10.00±1.00[f]	22.00±0.00 [f]	40.00±5.00 [f]
Total E-Coli Count(cfu)	0	8.00±1.73[g]	13.00±4.58 [h]	23.00±2.65 [g h]

Values are mean±Standard deviation of triplicate determinations values bearing the same superscript "a,b,c,d,e,f,g,h" across the same row are significantly different (p<0.05).

3.2 Discussion

The mean pH values recorded showed that ground water, upstream and downstream waters are slightly acidic and below the lower permissible limit recommended by WHO and FMENV. This may be due to the organic contamination which may come from natural leachates, atmospheric droplets and human contamination during fermentation of cassava in the water. Also caustic soda from soap and detergent during washing of cloths and bathing in the stream may be the cause of low pH as recorded in Ekhaise and Anyasi (2005).

The mean temperature of the water samples collected was within the permissible limit. Also Ekhaise and Anyasi (2005) reported that change in temperature difference of any aquatic habitat is affected by weather, the extent of shade from direct exposure to sunlight or biodegradation of organic matter that enter the water.

The mean values of conductivities of ground water is a little bit higher than WHO/FMENV limits while that of upstream and downstream waters are lower, though the waters can be suitable for domestic uses. The high conductivity value in the ground water may be due to high total dissolved solid as found in Akubugwu and Duru (2011).

Turbidity in drinking water is caused by particulate matter that may be present from water source as a consequence of inadequate filtration. From the mean values of turbidity of the waters, ground water is below the permissible limits while that of upstream and downstream waters were above the permissible limits and can shield the pathogenic organisms. Therefore, the higher the turbidity, the more energy and chemicals required for water treatment (Obasi *et al*., 2004).

The mean value of Dissolved Oxygen (DO) of ground water was within the limit of FMENV and a little bit higher than the WHO while that of upstream and downstream water are a little bit below the limit values recommended by WHO/FMENV and therefore can support aquatic life (Njoku-Tony *et al*., 2016). Though, Ukaga and Onyeka (2002) stated that the desirable range of dissolved oxygen for normal fish growth is between 5.5 to 7.8mg/L.

The total dissolved solid is indicative of material carried in solid form and this falls within the WHO/FMENV standards.

In Tables 1, 2 and 3 the mean chloride are 145.8mg/L, 72.9mg/L and 182.2mg/L which are quite lower than the WHO/FMENV limit of 250mg/L, the chloride of the upstream water was relatively higher than that of the ground water and downstream water which do not pose any health risk (WHO, 2011).

The water samples foam easily with soap. Comparatively, the upstream water sample had the lowest value of 0.6mg/L and will produce lather with soap easier than the downstream and ground water. The direct effect of hardness on human health is yet to be proven scientifically (Sharma and Chandel, 2004). Hardness is not a health concern but can cause mineral build-up in plumbing fixtures and poor foaming of soap and detergents (WHO, 2011).

From the mean values of Nitrate in Table 4 recorded lower compared with WHO and FMENV limits. This means that the nitrate levels of the three water samples do not pose any health threat. High concentration of nitrate in both surface and shallow groundwater can be probably due to poor sanitation and latrine construction, fertilizer and other agrochemical use and causes methemoglobinemia in children (Margaret *et al*., 2012).

The BOD values fall within the WHO standard. According to Moore and Moore (1976), BOD values of 1-2 mg/L was classified as clean water, 2-3 mg/L as fairly clean water, 4-5 mg/L as fairly polluted water and 10mg/L as bad and polluted water. Therefore, the ground water and upstream can be classified as fairly clean water while the downstream can be classified as clean water.

Results of the heterotrophic bacterial count showed that the ground water had the lowest load. This is simply a measure of the number of live bacteria present in water and does not necessarily indicate health threats. Faecal coliform bacteria were detected in all the waters but were a bit much in the downstream water. According to FMENV standards, drinking water should have zero faecal coliform bacterial count in 100ml of the water. It is most likely that faecal contamination arises from human activities. The mean values of *E. coli* detected (0.8×10^1Cfu/ml) in the ground water, (1.3×10^1cfu/ml) in the upstream water and (2.3×10^1cfu/ml) in the downstream water. *E. coli* is normally a harmless commensal in the alimentary canal of a man and other animals. However, some sero-types frequently cause gastroenteritis characterized by severe diarrhea with mucus or blood and with dehydration but usually without fever. Children, especially the newborn are usually affected but increasing cases of adult diarrhea caused by *E. coli* are also being noted (Okafor, 1985). Therefore, the presence of *E. coli* in the waters makes it potential health risk to its consumers.

4 Conclusion

Due to the heavy bacterial load, the water sampled were not good drinking and for other domestic activities. There is need to reduce most anthropogenic activities around the water source especially those that have negative impact on the water body such as defecation (both humans and animals), fermentation etc. This will help to improve the sanitization of water for domestic use since the stream and ground water are the major source of water in this area. Furthermore, sinking of shallow borehole should be discouraged.

REFERENCES

[1] Akubugwo E. I. and Duru M. K. C. (2011). Human Activities and Water Quality: a case study of Otamiri River, Owerri, Imo State Nigeria. *Global Research Journal of Science.* 1: 48-53

[2] APHA (2005). *Standard Methods for the Examination of Water and Wastewater*. 21st ed. American Public Health Association. Washington DC. 46.

[3] Ekhaise F. O. and Anyasi C. C. (2005). Influence of Breweries Effluent Discharge on the Microbiological and Physico-chemical Quality of Ikpoba River, Nigeria. *African Journal of Biotechnology.* 4(10): 1062-1065.

[4] Moore W. T. and Moore E. A. (1976). *Environmental Chemisty.* Academic Press London. 360-368.

[5] Margaret M., Nancy M. T., Keith S. P. and Robert J. N. (2012). Nitrate: Health Effects in Drinking Water. Natural Resources;Cornell cooperative Extension. www.psep.ice.cornell.edu.

[6] Njoku-Tony R. F., Ebe T. E., Ihejirika C. E., Ejiogu C. C. and Uyo C. N. (2016). Assessment of Physico-chemical and Microbial Load of Nworie River, Owerri, Imo State, Nigeria. *Journal of Mobile Computing and Application.* 3(1): 29-37.

[7] Obasi R. A, Balogun O. and Ajayi O. (2004). The Physico-chemical Investigation of River Irejo, Ekiti State, Nigeria. *Journal of Applied Science.* 7(2): 4121-4334.

[8] Okafor N. (1985). *Aquatic and Water Microbiology*. Fourth Dimension Publishing Ltd., Enugu p. 87.

[9] Sharma S. K. and Chandel (2004).Groundwater Pollution and Evaluation of Physico-chemical Properties of Groundwater. *Environmental and Ecology* 2 (2):319-324.

[10] Ukaga C. N. and Onyeka P. I. K. (2002). *Aquarium and Hydrobiology Techniques in Biology.* 1st ed. Optimal International Ltd, Enugu. Pp 144-149.

[11] WHO, (2011). Guidelines for Drinking Water Quality. Geneva.

[12] WHO, (2008). Guideline for Drinking Water Quality.First Addendum to third Edition. World Health Organisation, Geneva. 515.

SOCIETY FOR SCIENCE AND EDUCATION
UNITED KINGDOM

JBEMi JOURNAL OF BIOMEDICAL ENGINEERING AND MEDICAL IMAGING

ISSN: 2055-1266
VOLUME 5 ISSUE 3

Advanced Ambulatory Operating Stretcher Learned by Means of Convulational Neural Network (CNN)

[1]Sariena Talpur, [2]Nazaruddin Khoso
[1,2]Institute of biomedical engineering and technology, Liaquat University of medical and health sciences, Jamshoro Sindh Pakistan
sarienatalpur@gmail.com ;14bme22@gmail.com

ABSTRACT

According to scientists transportation is the major problem in today's world. The paper presents a method to transferring the patient from long distances or even from shorter distance. Concerned people face many problems in transferring the patient from one place to another place even from ambulance to stretcher or from stretcher to bed and vice versa. Some of the time it is difficult to move the stretcher because of the heavy weight of the patient, It requires more than two or three person in engaging the stretcher while in transferring patient. It will also cause un-peaceful conditions in the hospital and also it will effect on patient's health too.

We tried to overcome these problems via Transfer learning with the help of convolutional neural network in order to move the patients. This type of stretcher solve the problem through self-operating stretcher instead of it operates manually.

Keywords: stretcher, ambulatory system, transporting device, ambulance, convolutional neural network.

1 Introduction

As the very first we know that stretcher is one of the priority basis need for every hospitals, in order to move patient from ambulance to the stretcher and from stretcher to the respective bed and vice versa [1-4,6-7]. Therefore this is a most essential need for medical aid system. Whenever the emergency occur it causes disturbance in shifting the patients on to the stretcher and stretcher is take it by two or more person in order to reach to its destination place in the hospital [5,8-10]. These will all creates massive disturbance in the hospital environment too.

Advanced ambulatory stretcher system is an itself complete device which can gives self-control mobility to the hospitals rather than involvement of any medical staff members. Most of the stretchers can operate on the buttons, hydraulic system or even by the pressure system to control movements and motion of the stretcher [11,14,16]. This advanced ambulatory stretcher system is totally based on the artificial intelligence. This system will recognize the objects, person or any distortion that will disturb its path with the help of qualified trained model. Along with this feature it also has small touch screen system that is used to select respective destination in the hospital. By using the transfer learning with

DOI: 10.14738/jbemi.53.4660
Publication Date: 26th June 2018
URL: http://dx.doi.org/10.14738/jbemi. 53.4660

MATLAB software we train the stretcher with convolutional neural network technique along with pre-trained ALEXNET model. First it will train then all the movements (right, left, forward, backward, lifting, brake system, horn system) will occur automatically by means of artificial intelligence.

2 Methodology

To make the advanced stretcher it consists of four motors for the wheels of the stretcher to provide necessary transportation. The stretcher uses external energy to work therefore we provide the 12 volt battery to the stretcher in order to move it into particular direction. It also uses camera module so that it will recognized the objects.

2.1 Training of the Stretcher

ConvNET or CNN (convolutional neural network) is known as one of most famous and successful algorithm for the images and video with deep learning. Similar to the other networks of neural network, CNN is also composed of three layers input layer, output layer and hundreds and thousands of the hidden layers to acquire the greatest accuracy.

For training the images, CNN uses two of its layers:

- Feature detection layer
- Classification layer

2.1.1 Feature Detection Layer

This layer of CNN is consisting of three operations for the purpose to detect the feature of the images or data and perform either one of them.

2.1.1.1 Convulution: It takes input data and applies on them through set of convolutional filters; each filter of convolutional activates respective features from the images.

2.1.1.2 Pooling: Simply identify the output by taking non-linear sampling from input and also reduces other parameters needed for the network to learn about.

2.1.1.3 Rectified Linear Unit(Relu): This the most effective method and also faster than others methods. This is trained by mapping out all –ve values to zero and keep maintaining all +ve values.

These all methods are repeated continuously to hundreds and thousands of the hidden layers to detect features of the input and dataset.

2.1.2 Classification Layer of CNN

After passing through feature layer, CNN shift to the next and final layer known as classification layer, whose output is K dimension vector which represent the number of classes on the training dataset, that network used to predict.

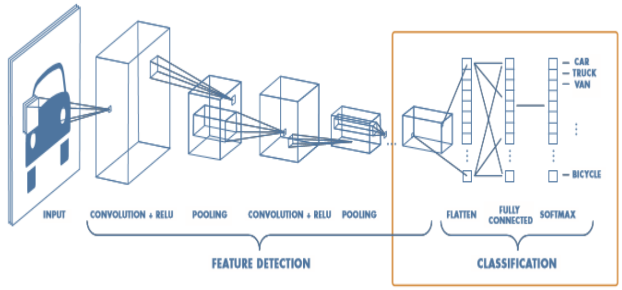

Figure 1: Model of CNN (convolutional neural network)

And we used pre-trained ALEXNET model to makes some changes with the 1st and last three layers for the new dataset of the images. The selection of this model is that it has ability to trained millions of the image at one time and classifies these images into 1000 objects.

Table I: Description of 25 layers of convolution neural network, bold layers indicates working layers.

LAYERS = 25X1 LAYER ARRAY WITH LAYERS:			
1	'data'	Image Input	227x227x3 images with 'zerocenter' normalization
2	'conv1'	Convolution	96 11x11x3 convolutions with stride [4 4] and padding [0 0 0 0]
3	'relu1'	ReLU	ReLU
4	'norm1'	Cross Channel Normalization	cross channel normalization with 5 channels per element
5	'pool1'	Max Pooling	3x3 max pooling with stride [2 2] and padding [0 0 0 0]
6	conv2'	Convolution	256 5x5x48 convolutions with stride [1 1] and padding [2 2 2 2]
7	'relu2'	ReLU	ReLU
8	'norm2'	Cross Channel Normalization	cross channel normalization with 5 channels per element
9	'pool2'	Max Pooling	3x3 max pooling with stride [2 2] and padding [0 0 0 0]
10	'conv3'	Convolution	384 3x3x256 convolutions with stride [1 1] and padding [1 1 1 1]
11	'relu3'	ReLU	ReLU
12	'conv4'	Convolution	384 3x3x192 convolutions with stride [1 1] and padding [1 1 1 1]
13	'relu4'	ReLU	ReLU
14	conv5'	Convolution	256 3x3x192 convolutions with stride [1 1] and padding [1 1 1 1]
15	'relu5'	ReLU	ReLU
16	pool5'	Max Pooling	3x3 max pooling with stride [2 2] and padding [0 0 0 0]
17	'fc6'	Fully Connected	4096 fully connected layer
18	'relu6'	ReLU	ReLU
19	drop6	Dropout	50% dropout
20	'fc7'	Fully Connected	4096 fully connected layer

21	'relu7'	ReLU	ReLU
22	drop7'	Dropout	Dropout
23	'fc8'	Fully Connected	1000 fully connected layer
24	'prob'	Softmax	Softmax
25	'output'	Classification Output	crossentropyex with 'tench', 'goldfish', and 998 other classes

After loading trained model of ALEXNET webcam/camera capture live pictures to identify the distortions like person or objects which can disturb its path.

It used camera /webcam to classify object or data and this all done with MATLAB along with

- Neural network toolbox.
- Support package for using webcam in MATLAB.
- Support package for using ALEXNET.
- LABVEIW along with LEGO MINDSTORM support package.
- Designed stretcher.

2.2 Programming (VI) for the Stretcher

To control the stretcher by means of computer it needs software known as LABVEIW 7.1 with LEGO MINDSTORM® NXT software for its programming for giving different direction to the stretcher.it is responsible for the movements.

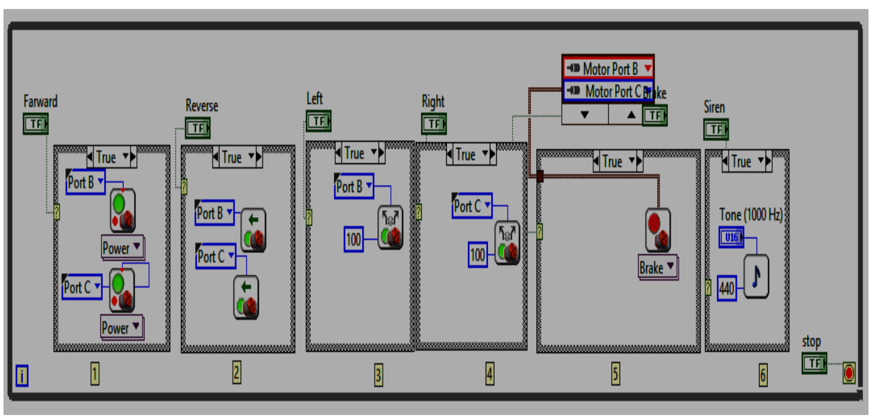

Figure 2: Programming sketch on LabVIEW

This is a complete visualization of programing

Its programming is consist of six sub blocks

- o First block is concerned with movement in forward direction. Port B and Port C represent attachment port for respective motors.
- o Second block represent movements in backward direction.
- o Third and fourth blocks are responsible for left and right movements.
- o Fifth block responsible for braking system whenever obstacle comes in path of stretcher it will stop its movements with help of this block.

- Sixth and last block is indicating alarming. When obstacle comes in front of the stretcher it will stop and start alarming.

2.3 Method for Working

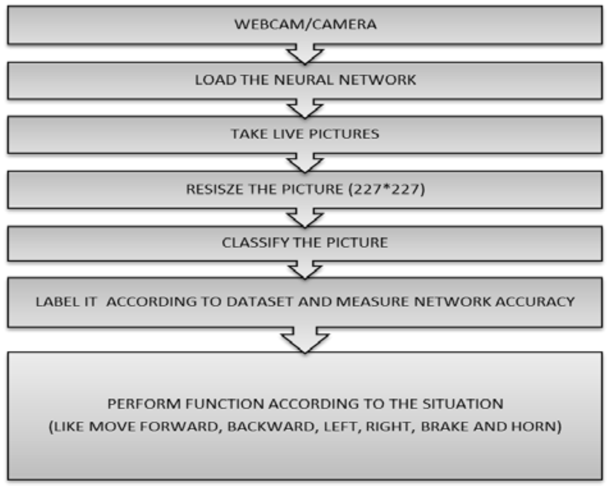

Figure 3: Block diagram showing working principle of CNN based stretcher

3 Algorithm Architecture

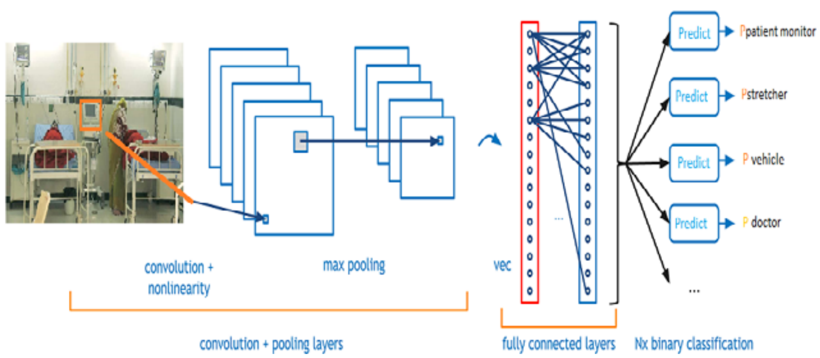

Figure 4: Showing that how CNN based stretcher recognized the objects

Here we have collected thousands of images from hospitals and make a complex dataset of images and to train this dataset and makes trained model for new live images as kernel get predict. The function which we used that is Softmax because it has good accuracy for images dataset instead of others.

$$Y = softmax\,(X.W + b) \tag{1}$$

Where

Y = Prediction (Output)
Softmax = Function
X = Input images (227*227*3)
W = Weight
B = Bias

4 Experiment and Analysis

Experiments are performed as

- First it will capture live images of the object with the help of camera module.
- Then it recognized the images and decides according to the given condition.

4.1 Results

(a) (b)

Figure 5: Indicates the detection of different objects

5 Conclusion

Advanced self-operating stretcher system itself has a self-controlling power and self-decision making power. It is suitable for every hospital in the world. This type of stretcher reduces staff stress, maintain environment of the hospitals, reduces the need of staff members to carry stretcher and does not create any massive conditions that will creates any disturbance. This is a complete package needed for every hospital and in the field of health care.

REFERENCES

[1] Nitin G. Sushir, Ravi B. Bopche, Prof. Hemant M. Bansod, "Design and Fabrication of Wheelchair cum Stretcher" Research Association of Masters of Engineering, Vol:4, pp.6-11, 2017.

[2] Wadgure, A. T., Deshmukh, S., & Vaidya, R. D. (2014). Development of Modified Mattresses for Patient Handling in Hospital. International Journal of Engineering Trends and Technology, 8(7), 354-358. Doi:10.14445/22315381/ijett-v8p264

[3] Design and Devolvement of modified mattresses for patient handling in hospital. ISSN 2278-0149, VOL 2, NO.4, OCT 2013.

[4] Modeling of modified mattresses for patient handling in hospital. ISSN 2319 – 7293, G.J.E.D.T., Vol. 2(5):41-44. (SeptemberOctober, 2013)

[5] Kevin Hsu ET all fall 2008, a design of Portable Lift for Transferring Wheelchair patients to Elevated Vehicle/ ambulance, University of Michigan Orthotics and Prosthetics Centre.

[6] Ehsanullah Khan et al., Synthesis of Trolley cum Wheelchair for Patient Handling, International Journal of Engineering, Science and Technology (IJEST) Vol.3 No.8, Aug.2011 Pgs.6311-6316.

[7] Wei Ching-Hua et all Nov. 5-8 2007, Hospital bed with Auxiliary Functions of Lateral and Transferring for Immobilized patients Taipei, Taiwan. The 33rd Annual Conference of the IEEE Industrial Electronics Society (IECON) Pgs.2991-2995.

[8] Tiernan John et al., A Survey of the Wheelchair and Seating Market in Irelands, Assistive Technology-shaping the future; AAATE conference proceedings, Vol. 11. No. 1 Pgs- 105-111.

[9] Wadgure, 2(11): November, 2013] ISSN: 2277-9655 Impact Factor: 1.852 http: //www.ijesrt.com(C)International Journal of Engineering Sciences & Research Technology [3268-3273]

[10] Wei Ching-Hua et al. (November 5-8, 2007), "Hospital Bed with Auxiliary Functions of Lateral and Transferring for Immobilized Patients Taipei, Taiwan", The 33rd Annual Conference of the IEEE Industrial Electronics Society (IECON), pp. 2991-2995.

[11] Hongbo Wang and Fumio Kasagami, A Patient Transfer Apparatus Between Bed and Stretcher, IEEE transaction on System, Man, and Cybernetics-part-B:, Vol. 38,No.1, Feb.2008.

[12] Rao J. S. 'Mechanism and Machine Theory'- New Age International (p) Ltd Publisher, Edition 2.

[13] Shigley's Mechanical Engineering Design, McGraw-Hill Primis Online, Budynas−Nisbett, Edition 8.

[14] Lesley, Samuel, Porter & Lucy A, "An Ergonomics Wheelchair for Hemiplegics" Technology & Disability, Vol.14 No. 4, Pgs 183-189, Publication 2002.

[15] ACEP. New equipment guidelines. Emergency Medical Services. 2001; 30: 42

[16] Alberti G, Cooke M. Ambulance improvement check list.

[17] Allen M. Creating crew space – ambulance modifications for medics. Journal of Emergency Medical Services. 1997; 22: 66-67